MATHEMATICAL REGRESSION MODELING OF THE LASER DIRECT METAL DEPOSITION PROCESS FOR INCONEL 718

Nguyen Van Toan[1], Mai Xuan Hai[1], Doan Tat Khoa[1,*]

DOI: https://doi.org/10.57001/huih5804.2026.121

ABSTRACT

This paper presents a comprehensive mathematical regression analysis of the Direct Laser Metal Deposition (DLMD) process for Inconel 718, with the aim of quantifying the relationships between key process parameters and coating geometrical characteristics. Laser power, scanning speed, and powder feed rate were selected as the primary process variables. A series of designed experiments was conducted, and polynomial regression models were established to describe the effects of both individual parameters and their interactions on coating geometrical characteristics, including width, height, and dilution. The ANOVA results revealed high coefficients of determination for clad height ($R_1^2 = 0.9858$), clad dilution ($R_2^2 = 9669$), and clad weight ($R_3^2 = 0.907$), confirming the excellent fitting accuracy and predictive capability of the proposed models. Among the investigated process parameters, laser power was identified as the dominant factor influencing clad geometry, whereas scanning speed and powder feed rate exhibited comparatively minor effects. In summary, the developed regression equations demonstrated high predictive accuracy, enabling reliable estimation of optimal parameter ranges for producing dense and dimensionally stable Inconel 718 deposits.

Keywords: *Direct laser metal deposition, Inconel 718, Response Surface Methodology.*

[1]Faculty of Mechanical Engineering, Le Quy Don Technical University
[*]Email: doankhoactm@gmail.com
Received: 01/3/2026
Revised: 28/4/2026
Accepted: 25/5/2026

1. INTRODUCTION

Direct Laser Metal Deposition (DLMD) has emerged as a leading method for producing and repairing metal parts with exceptional mechanical properties and metallurgical integrity [1, 2]. In DLMD, a high-power laser beam melts metal powder, which is fed coaxially into the melt pool, allowing for precise control of microstructure, density, and dimensional accuracy [3].

Inconel 718 is a nickel superalloy, which is one of the most widely used materials for high-temperature and corrosion-resistant applications due to its superior strength, creep resistance, and fatigue performance up to 700°C. However, its poor machinability and high work-hardening rate make conventional manufacturing methods inefficient and costly [4]. Despite its advantages, achieving optimal mechanical and geometric quality in DLMD-fabricated Inconel 718 remains a major challenge because of the complex interrelationships among process parameters [1]. The primary process parameters in DLMD are laser power, scanning speed, powder feed rate, layer/hatch spacing, focal offset, scanning strategy, and substrate-preheat or assist gas conditions. It is essential to understand how these parameters influence key responses avariable such as deposition geometry, build stability, microhardness, microstructural features, and defect levels [5, 6].

Most previous studies have investigated and optimized the DLMD process via conventional experimental approaches [7, 8]. However, such methods are often time-consuming, costly, and labor-intensive due to the large number of required trials. Moreover, these studies primarily examined the individual effects of process parameters, neglecting their interactive influences, which can lead to significant unexplained variability and limit industrial applicability. Recent studies have demonstrated the potential of Response Surface Methodology (RSM) in optimizing DLMD parameters for nickel-based superalloys. For example, Shayanfar et al. [7] used a central composite design to model the effects of laser power, powder feed rate, and scanning speed on clad height and microhardness of Inconel 625, achieving significant improvements in deposition uniformity. Similarly, Eden Amar et al. [9] applied RSM to optimize Inconel 316L for DLMD parameters, revealing that laser power and powder mass flow rateh ave the most

significant effects on single-layer height. These findings confirm that RSM not only reduces experimental costs but also enhances process predictability, providing a systematic route toward data-driven optimization of DLMD processes. Accurately predicting the properties of an individual coating layer is of critical importance. We have tried to build an empirical statistical relation for the laser cladding of Inconel 718 powder on SS 316L steel substrate using a regression method, and a statistical model for predicting the properties of cladding is proposed.

In this work, we employ RSM to develop an analytical prediction model of the combined effects and to assess the interactions among the key processing parameters (laser power (P), powder feed rate (F), and scanning speed (V)) and the deposited Inconel 718 geometrical characteristics responses.

2. EXPERIMENTAL

2.1. Description of the experimental setup

Figure 1a shows a schematic diagram of the experimental system, which consists of a fiber laser source, a powder feeding system, a deposition nozzle, and a three-axis CNC mechanism. Argon was employed as the shielding gas at a flow rate of 3L/min. Figure 1b indicates the fabrication principles of the DLMD process. The DLMD process demonstrates precise layer-wise material deposition, enabling complex geometries with controlled microstructure and enhanced mechanical properties. To have a dense powder stream for the direct laser metal deposition DLMD process, a brass coaxial nozzle is used. The powder particles were blown from four channels, which are designed to focus the powder particles in the powder concentration plane. Fig. 1c illustrates the powder stream convergence zone of the powder stream under the powder coaxial nozzle. The powder flow convergence point was recognized 15mm under the powder coaxial nozzle. The track deposition process was performed in an Ar atmosphere to minimize oxidation during fabrication. The O_2 level inside the closed chamber was maintained below 5ppm throughout the deposition process. The gas circulation system was kept operating, with shielding gas blowing onto the substrate during the dwell time. The experimental plan was developed by keeping as constant the carrier gas flow rate constant for all the experiments.

In this work, Inconel 718 powder was deposited on SS 316L steel substrate using DLMD process. The substrates were prepared into flat rectangular samples with dimensions of (200x100x10) mm was used as the substrate. The Inconel 718 powder was used as the feedstock powder. The chemical composition of the Inconel 718 powder was inductively coupled plasma (ICP) analysis (ES-730; SpectroArcos-AMETEK. Table 1 shows the ICP analysis results of the chemical composition of the Inconel 718 powder. Inconel 718 powder used in the experiment had a particle size ranging from 15 to 55mm, with a standard deviation of 9.22mm.

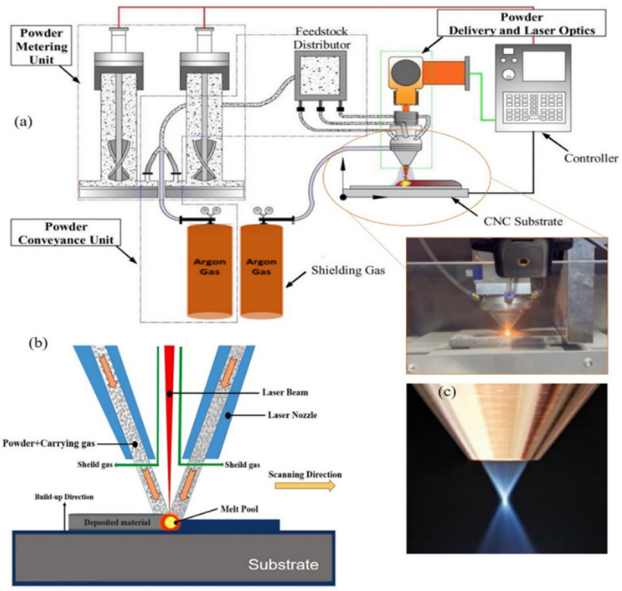

Figure 1. (a) Schematic diagram of the experimental setup, (b) the fabrication principles of the DLMD process, and (c) the image of the powder stream convergence zone of the powder stream under the powder coaxial nozzle

Table 1. Chemical composition of the Inconel 718 powder

Element	Ni	Cr	Fe	Nb	Mo	Al	Si	Mn	Ti	Co
Weight percentage (%)	55.2	18.6	17.4	4.7	3.29	0.247	0.2	0.163	0.13	0.07

The morphology of the powder particles was observed and analyzed by using scanning electron microscopy (SEM) (MIRA3, TESCAN instrument, Czech Republic) (as Figure 2). SEM imaging of Inconel 718 powder reveals particle morphology, surface texture, and sphericity, all of which strongly affect powder flowability and packing behavior during DLMD. The accompanying powder size distribution provides quantitative insight into particle uniformity. Together, these characteristics are critical for predicting process stability, melt behavior, and the final microstructural quality of DLMD-formed products. In order to prepare the samples for the DLMD process, the sample surfaces of the substrates were

ground by a grinding machine to have a smooth surface to decrease the samples' surface roughness by 0.8μm. Before conducting the DLMD experiments, by using acetone, the grease and residue on the surface of the base metal were removed, and also the oxidation film was removed with a stainless steel brush.

In this work, the main input parameters of the DLMD were laser scanning rate V (mm/s), powder feeding rate F (mg/s), and laser power P(W) and the output parameter were selected as the width of the weld (W(μm)), the height of the cladding layer (H(μm)), and the depth of penetration relative to the cross-sectional area of the deposited track and the melt pool. The samples were polished and etched with a solution with equal parts of HCl, HNO_3, and CH_3COOH. Afterwards, they were imaged by a scanning electron microscope (FESEM; MIRA3; Czech Republic).

2.2. Mathematical regression method

A mathematical regression method based on response surface methodology (RSM) was used to establish the relationship between the independent variables, including the laser scanning speed (V (mm/s) (or x_1), laser power (P(W)) (or x_2), and powder feeding rate (F (mg/s) (or x_3), and response variables, such as the coating geometries (width, height, depth of penetration and dilution). Table 2 lists the variable factors and the corresponding factor levels used for the deposition of Inconel 718 experimental matrix. The key parameters that must be controlled to ensure an effective laser deposition process, applicable to both cladding and additive manufacturing, are the clad height (H(μm)), width (W(μm)), and dilution (D(%)). The dilution analyzes the ratio between the molten base material and the deposited material and is typically calculated as using Eq. 1 [10].

$$D(\%) = \frac{A_m}{A_m + A_c} \quad (1)$$

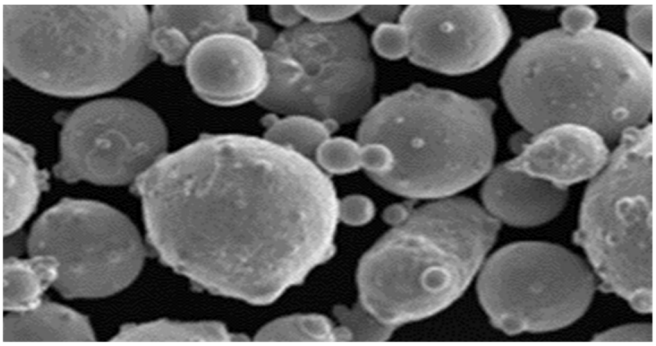

Figure 2. The SEM image of Iconel 718 powder

Table 2. DLMD processing parameters and their corresponding levels

Parameters	Units	Level of parameters		
		level-1	level 0	level +1
Scanning speed (V)	mm/s	3	4	5
Laser power (P)	W	250	300	350
Powder feeding rate (*F*)	mg/s	100	200	300

To evaluate the statistical significance of the effects of the process parameters on the final quality of the deposited clad, an analysis of variance (ANOVA) based on a general linear model was employed. A three-factor, three-level central composite design (CCD) and a quadratic regression model were employed to characterize the interactions between the process variables and the corresponding response variables [9]. Table 3 indicates the experimental matrix together with the corresponding analytical response data.

The effects of the independent variables on the response variables, including contour plots and response surface plots, were generated using Design-Expert Software 12 (DoE, Stat-Ease Inc., USA). The influences of the operating parameters on the response variables were examined in detail using Eq. (2):

$$Y = \beta_0 + \sum_{i=1}^{k} \beta_i x_i + \sum_{i=1}^{k} \beta_{ii} x_i^2 + \sum_{i=1}^{k-1} \sum_{j=i+1}^{k} \beta_{ij} x_i x_j \quad (2)$$

where Y represents the predicted or output variables; are the input variables; $x_i^2, x_j^2, ..., x_k^2$, denote the quadratic effects; $x_i, x_j, x_i x_k, ..., x_j x_k$ represent the interaction effects; and β_0, β_i,..., β_{ij} are the estimated regression coefficients.

Table 3. Experimental design matrix and observed values based on the central composite design (CCD) used in this study

Run order	Codes values (x)			Experimental data Responses (Y)			Predicted value		
	x_1	x_2	x_3	H (μm)	D (%)	W (μm)	H′ (μm)	D′ (%)	W′ (μm)
1	4	300	100	88.2	50.03	1648.1	89.16	49.25	1599.17
2	4	300	200	108.3	38.64	1561.5	108.38	39.65	1573.53
3	4	300	200	101.6	39.09	1558.8	108.38	39.65	1573.53
4	3	300	200	185.2	33.02	1685.1	166.02	33.19	1633.45
5	3	350	100	220.3	37.18	1783.5	215.11	38.41	1769.85
6	3	350	300	228.4	34.12	1758.4	244.1	32.24	1718.57
7	3	250	300	138.3	28.53	1465.3	135.21	30.42	1497.05
8	5	350	300	151.1	40.61	1658.6	141.87	42.49	1598.73

9	4	300	200	105.1	39.01	1548.5	108.38	39.65	1573.53
10	4	300	200	103.2	39.83	1546.1	108.38	39.65	1573.53
11	4	300	200	106.5	38.76	1552.3	108.38	39.65	1573.53
12	5	300	200	70.3	49.35	1446.7	79.34	47.25	1513.61
13	4	300	300	139.3	38.25	1528.3	128.2	37.1	1547.89
14	3	250	100	116.3	36.99	1512.3	128.07	35.59	1548.33
15	4	300	200	105.3	38.71	1554.2	108.38	39.65	1573.53
16	5	250	300	98.3	36.04	1388.5	106.03	35.3	1377.21
17	4	250	200	95.2	36.71	1527.4	91.96	34.59	1462.77
18	4	350	200	160.3	39.42	1635.4	153.4	39.6	1684.29
19	5	250	100	70.1	51.08	1473.2	56.94	53.45	1428.49
20	5	350	100	65.3	63.04	1638.4	70.93	61.64	1650.01

3. RESULTS AND DISCUSSION

3.1. Statistical analysis and the model fitting

A multivariate regression model was developed to describe the relationship between the output responses and the operating parameters. Three coded levels (−1, 0, and +1, corresponding to low, medium, and high factor values) were assigned to each of the three selected variables (Table 2). The coefficients of the resulting polynomial equations were estimated from the experimental data using the central composite design (CCD) (Table 3), allowing for the analysis and prediction of the response variables. Table 3 also reports both the predicted and experimental geometrical characteristics, demonstrating a strong concordance between measured and model-predicted values. Furthermore, the experimental dataset was subjected to analysis of variance (ANOVA) to determine the significance of the regression terms and to calculate the coefficients of the polynomial equations.

The regression equations for each response variable obtained from the response surface methodology (RSM) are presented in Eqs. (3) - (5).

$$\begin{aligned} H = {} & +514.33 - 69.14x_1 - 1.5751x_2 - 0.564x_3 \\ & - 0.36525x_1x_2 + 0.1048x_1x_3 + 0.001093x_2x_3 \\ & + 14.3x_1^2 + 0.00572x_2^2 + 0.00003x_3^2 \end{aligned} \quad (3)$$

$$\begin{aligned} D = {} & -56.699 + 0.8808x_1 + 0.5655x_2 - 0.0572x_3 \\ & + 0.02686x_1x_2 - 0.03243x_1x_3 - 0.00005x_2x_3 \\ & + 0.5717x_1^2 - 0.00102x_2^2 + 0.000353x_3^2 \end{aligned} \quad (4)$$

$$W = +1199.93 - 59.92x_1 + 2.2152x_2 - 0.2564x_3 \quad (5)$$

The statistical analysis performed using ANOVA for the regression models corresponding to Eqs. (3) - (5) provides strong evidence for the suitability and robustness of the proposed quadratic polynomial model. The high coefficients of determination (R^2 = 0.9631 for The height of the cladding layer (H(μm)), R^2 = 0.9669 for Geometrical dilution (D) and R^2 = 0.907 for The width of the cladding layer (W(μm)) demonstrate that the majority of variations in the responses of 96.31%, 96.69% and 90.07%, respectively, which are effectively explained by the selected independent variables. The P-values, all below the 0.05 significance threshold, further confirm that the model terms are statistically meaningful relative to pure error, thereby validating the reliability of the fitted model. Additionally, the proximity of R^2 values to unity, together with the strong agreement between predicted and experimental data, indicates that the quadratic polynomial formulation adequately captures the influence of operational variables on the system responses. This confirms the model's predictive capability and its suitability for optimization. The statistical indicators further reinforce the robustness of the developed regression models.

3.2. Effects of input parameters on the clad height

The clad height is a critical geometrical feature in laser deposition, influencing the accuracy of fabrication in the vertical direction. As highlighted in [11], this parameter plays a significant role in controlling deposition quality. The clad height is closely related to the amount of powder injected into the melt pool, as indicated in [12]. The powder feeding rate and its spatial distribution within the laser interaction zone are key factors that significantly influence the clad height, directly affecting deposition quality and precision. The corresponding results are summarized in Table 3 and Figure 3. As illustrated in Figures 3(a-d), the surface plots depict the combined influence of these variables on clad height. The findings indicate that increasing the scanning speed exerts a negative effect on clad height. Specifically, a higher scanning speed decreases the interaction time between the heat source and the substrate, thereby limiting molten material deposition and ultimately reducing the resultant clad height.

The interaction between the laser beam and the powder flow is critical to deposition quality. As the nozzle moves along the substrate, the powder flow achieves to focuses on the top surface of the substrate. The substrate returned to being shadowed from the powder flow, and the absorption of the laser energy was better distributed between powder and substrate, increasing the clad height and deposition stability.

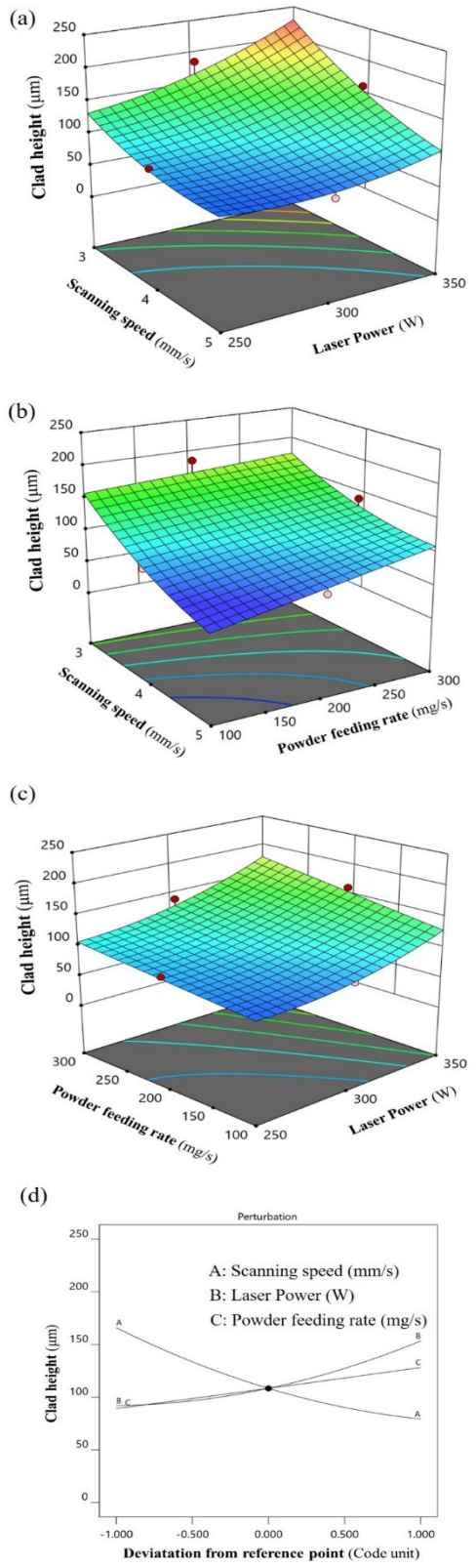

Figure 3. Three-dimensional response surfaces illustrating the effects of the independent variables: (a) scanning speed and laser power, (b) scanning speed and powder feeding rate, (c) powder feeding rate and laser power, and (d) the perturbation plot showing the influence of the three factors on the clad height

3.3. Effects of input parameters on the clad width

Figure 4 and Table 3 show a strong agreement is observed between the experimental trends and the predictions generated by the model, indicating that the proposed approach effectively captures the underlying process behavior. This consistency demonstrates the model's capability to reliably represent the evolution of clad width under varying operating conditions.

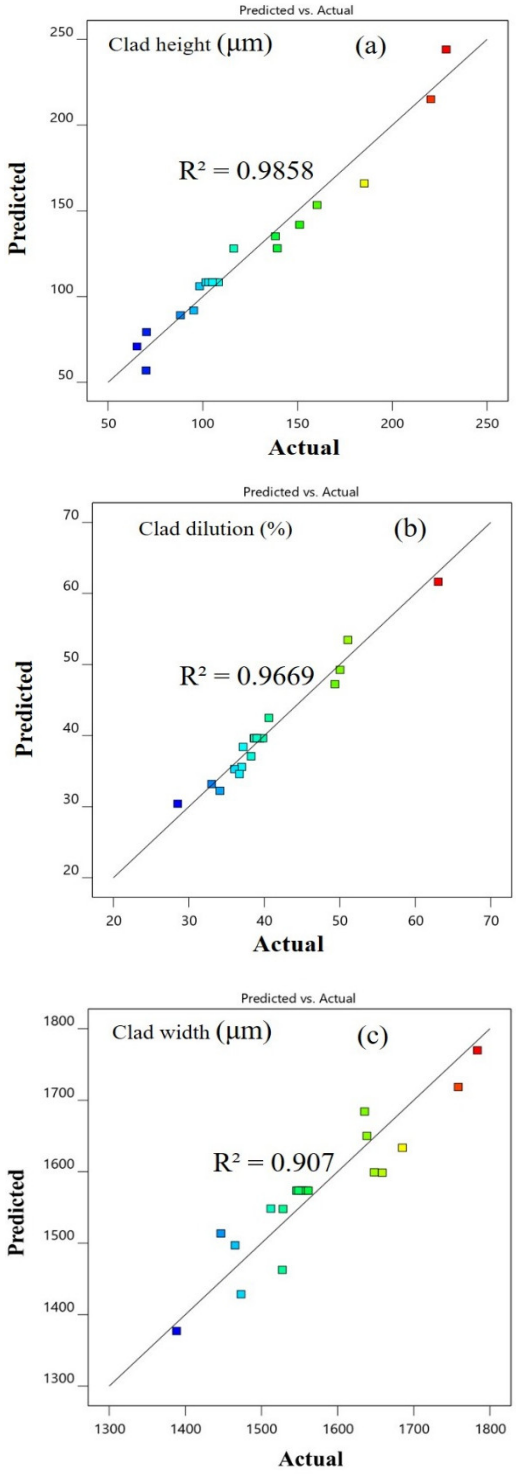

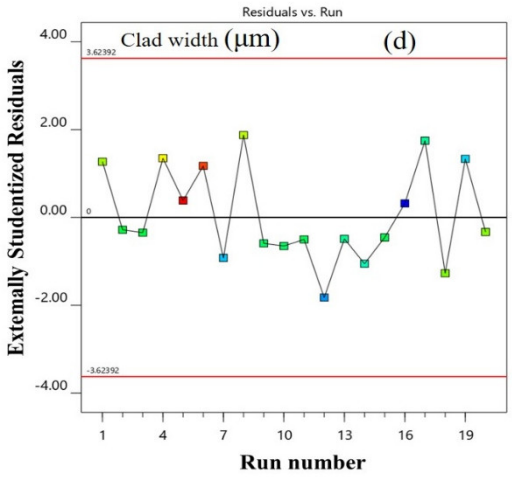

Figure 4. The plot of predicted value versus actual values for (a)clad height, (b)clad dilution, and (c) clad width, (d) the residuals vs. order of the data for clad width

Figure 4(a-c) presents a comparison between the experimental measurements and the predicted values obtained from the RSM mathematical model for clad height, clad dilution, and clad width. In all plots, the predicted values closely follow the diagonal line, indicating strong agreement between the model predictions and experimental measurements.

For clad height (Figure 4a), the data points are tightly clustered around the diagonal, with a coefficient of determination of R^2 = 0.9858, demonstrating high predictive accuracy. Similarly, clad dilution (Figure 4b) exhibits minimal scatter (R^2 = 0.9669), reflecting reliable model estimation. For clad width (Figure 5c), although a slightly larger deviation from the diagonal is observed at higher values (R^2 = 0.907), the overall trend still indicates good predictive capability. Collectively, these results confirm that the developed predictive model effectively captures the key characteristics of the clad geometry. In addition, residual analysis and a comparison between the predicted and actual values were performed to evaluate the adequacy of the reduced quadratic model. The results of the residual analysis are presented in Figure 4b. The residuals exhibited an approximately linear pattern, suggesting that the errors were normally distributed. As shown in Figure 4a, no discernible patterns or unusual structures were observed in the plot of residuals versus predicted responses. Therefore, there was no evidence indicating violations of the independence or constant-variance assumptions.

3.4. Effects of input parameters on the clad dilution

The influence of the DLMD process parameters on dilution can be understood through an analysis of the laser-powder interaction. In terms of penetration depth, it is crucial to consider the entire trajectory of the powder particles as they travel toward the deposition plane. As the powder particles pass through the laser beam, they absorb a portion of the energy that would otherwise be directed to the substrate. This energy absorption alters the laser's penetration into the base material, which, in turn, affects the dilution value. Figure 5 shows the interaction effect of the input parameters on the clad dilution. Figure 5 presents the surface plot of the interactive effects of DLMD process parameters on dilution. As observation results, increasing laser power generally enlarges the melt pool and promotes deeper substrate melting, thereby increasing dilution. In contrast, higher scanning speed reduces energy input per unit length, limits melt-pool penetration, and consequently decreases dilution. Powder feed rate also plays a critical role: excessive feed can cool the melt pool and reduce dilution, while insufficient feed promotes deeper substrate melting and higher dilution.

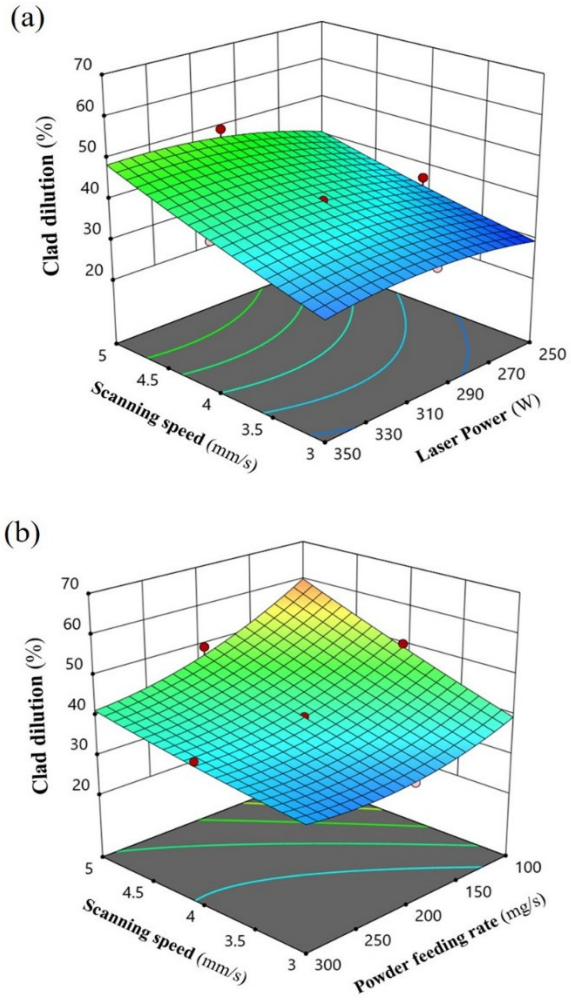

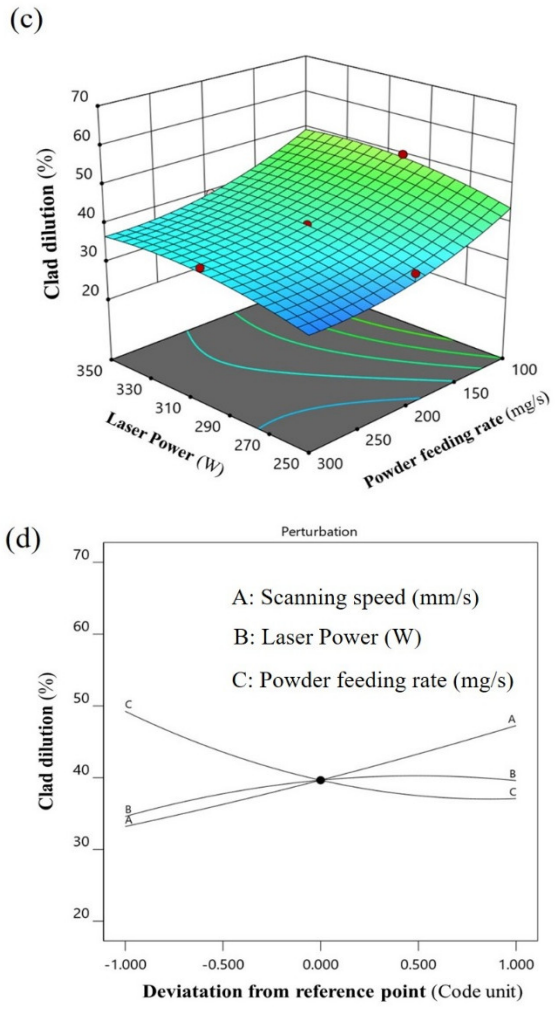

Figure 5. The responses plot of the effect of independent variables (a) scanning speed and laser power, (b) scanning speed and powder feeding rate, (c) laser power and powder feeding rate, and (d) the perturbation plot of the three factors on the clad dillution

4. CONCLUSION

This study developed a combined desirability function to evaluate the effects of multiple input parameters on the clad geometry in Direct Laser Metal Deposition (DLMD) using a Response Surface Methodology (RSM)-based mathematical model. Analysis of variance (ANOVA) demonstrated high coefficients of determination (R_1^2 = 0.9858 (clad height), R_2^2 = 9669 (clad dilution), and R_3^2 = 0.907 (clad weight)), indicating excellent model fitting and predictive capability. The results revealed that laser power is the most influential parameter affecting clad geometry, whereas scan speed and powder feed rate have relatively minor impacts. The strong agreement between the predicted and experimental values confirms that the RSM model can reliably simulate the practical outcomes of the DLMD process. By integrating multiple factors and responses into a single predictive framework, this approach enables fast, efficient, and accurate estimation of clad characteristics. Consequently, the proposed methodology provides a valuable tool for process optimization, reducing experimental trials while improving control over the geometric quality and reproducibility of deposited layers in complex DLMD applications.

REFERENCES

[1]. M. Moradi, Z. Pourmand, A. Hasani, M. Karami Moghadam, A.H. Sakhaei, M. Shafiee, J. Lawrence, "Direct laser metal deposition (DLMD) additive manufacturing (AM) of Inconel 718 superalloy: Elemental, microstructural and physical properties evaluation," *Optik (Stuttg),* 259, 2022.

[2]. P. Ghosal, M.C. Majumder, Anangamohan, C. Dhyay, "Study on direct laser metal deposition," *Mater. Today Proc.*, 12509-12518, 2018.

[3]. N. Shamsaei, A. Yadollahi, L. Bian, S.M. Thompson, "An overview of Direct Laser Deposition for additive manufacturing; Part II: Mechanical behavior, process parameter optimization and control," *Addit. Manuf.,* 8, 12-35, 2015.

[4]. M. Rahman, W.K.H. Seah, T.T. Teo, "The machinability of Inconel 718," *J. Mater. Process. Technol.* 63, 199-204, 1997.

[5]. N. Ndou, M.P. Mubiayi, "Effect of laser power and scanning speed on the characteristics of laser metal deposition of Ti6Al4V + W composite powder on Ti6Al4V substrate," *Mater. Res. Express*, 8, 2021.

[6]. C. Zhong, N. Pirch, A. Gasser, R. Poprawe, J.H. Schleifenbaum, "The influence of the powder stream on high-deposition-rate laser metal deposition with inconel 718," *Metals* (Basel), 7, 2017.

[7]. P. Shayanfar, H. Daneshmanesh, K. Janghorban, "Parameters Optimization for Laser Cladding of Inconel 625 on ASTM A592 Steel," *Journal of Materials Research and Technology,* 9, 4, 8258-8265, 2020.

[8]. A. Angelastro, S.L. Campanelli, G. Casalino, A.D. Ludovico, S. Ferrara, "A methodology for optimization of the Direct Laser Metal Deposition process," *Key Eng. Mater.,* 473, 75-82, 2011.

[9]. E. Amar, V. Popov, N. Eliaz, "Response Surface Methodology (RSM) Approach for Optimizing the Processing Parameters of 316L SS in Directed Energy Deposition," *Materials* (Basel), 2023.

[10]. D.T. Sarathchandra, M.J. Davidson, G. Visvanathan, "Parameters effect on SS304 beads deposited by wire arc additive manufacturing," *Mater. Manuf. Process.*, 1-7, 2020

[11]. K. Zhang, W. Liu, X. Shang, "Research on the processing experiments of laser metal deposition shaping," *Opt. Laser Technol.*, 39, 549-557, 2007.

[12]. M. Mazzarisi, et al., "Phenomenological modelling of direct laser metal deposition for single tracks," *The International Journal of Advanced Manufacturing Technology*, 111:1955-1970, (2020).